FERONIA receptor kinase pathway suppresses abscisic acid signaling in *Arabidopsis* by activating ABI2 phosphatase

Feng Yu[a], Lichao Qian[a], Candida Nibau[b,1], Qiaohong Duan[b], Daniel Kita[b], Kathryn Levasseur[b,2], Xiaoqian Li[a], Changqing Lu[a], Hui Li[a], Congcong Hou[c], Legong Li[c], Bob B. Buchanan[d,3], Liangbi Chen[a,3], Alice Y. Cheung[b], Dongping Li[a,3], and Sheng Luan[a,d,3]

[a]College of Life Sciences, Hunan Normal University, Changsha 410081, People's Republic of China; [b]Department of Biochemistry and Molecular Biology, University of Massachusetts, Amherst, MA 01003; [c]College of Life Sciences, Capital Normal University, Beijing 100037, People's Republic of China; and [d]Department of Plant and Microbial Biology, University of California, Berkeley, CA 94720

Contributed by Bob B. Buchanan, July 23, 2012 (sent for review February 16, 2012)

Plant growth and development are controlled by a delicate balance of hormonal cues. Growth-promoting hormones and growth-inhibiting counterparts often antagonize each other in their action, but the molecular mechanisms underlying these events remain largely unknown. Here, we report a cross-talk mechanism that enables a receptor-like kinase, *FERONIA* (*FER*), a positive regulator of auxin-promoted growth, to suppress the abscisic acid (ABA) response through activation of *ABI2*, a negative regulator of ABA signaling. The FER pathway consists of a FER kinase interacting with guanine exchange factors GEF1, GEF4, and GEF10 that, in turn, activate GTPase ROP11/ARAC10. *Arabidopsis* mutants disrupted in any step of the FER pathway, including *fer, gef1gef4gef10*, or *rop11/arac10*, all displayed an ABA-hypersensitive response, implicating the FER pathway in the suppression mechanism. In search of the target for the FER pathway, we found that the ROP11/ARAC10 protein physically interacted with the ABI2 phosphatase and enhanced its activity, thereby linking the FER pathway with the inhibition of ABA signaling.

A-type protein phosphatase 2C | signal transduction | small GTPase

Originally discovered as a hormone for senescence and abscission, abscisic acid (ABA) is generally considered an inhibitor of cell growth (1, 2). In addition, ABA plays a central role in plant stress responses. The content of ABA in plant cells significantly increases under drought or salinity stress conditions, inducing stomatal closure and gene expression to cope with stress conditions (3–5). Stress adaptation often involves the inhibition of vegetative growth, consistent with the known role of ABA. Recent work has identified several putative ABA receptors (3–5), in particular, the PYR/PYL/RCAR proteins linking ABA perception to a biochemical pathway consisting of A-type protein phosphatase 2Cs (PP2Cs) and SNF1-related protein kinase 2 (SnRK2)-type protein kinases (6–9). It is widely accepted that ABA binding to PYR/PYL/RCAR proteins initiates physical interaction and inhibition of PP2Cs, negative regulators in ABA signaling (3–5). Deactivation of PP2Cs releases SnRK2 kinases from the PP2C–SnRK2 complexes, activating those kinases that target proteins downstream.

While this primary "linear" pathway was being defined, parallel studies suggested that ABA signaling is regulated by a number of other pathways initiated by hormones and environmental factors (3, 4). However, little is understood about the molecular links that allow these alternate signaling pathways to intercept the primary ABA signaling pathway. We report that the *FERONIA* (*FER*) receptor kinase pathway, a signaling module that is required for auxin response (10), suppresses ABA signaling through activation of ABI2, a PP2C member located in the primary signaling pathway of ABA response.

Results and Discussion

***fer* Mutants Are Hypersensitive to ABA.** Receptor-like protein kinases (RLKs), which contain an extracelluar receptor domain and a cytosolic Ser/Thr kinase domain, function in a number of signaling processes in response to hormones and environmental factors (11). In previous work, we studied the transcriptional activity of a diverse superfamily of 604 RLKs associated with hormones and environmental stress (12). In particular, in an attempt to connect RLK-mediated signaling with hormonal responses, we focused on those RLKs that are highly regulated by hormones. We identified *FER* as one of the RLK members that displayed opposing expression patterns after treatment of *Arabidopsis* seedlings with auxin and ABA: *FER* mRNA was up-regulated by auxin and down-regulated by ABA. This finding was confirmed by available online databases and quantitative RT-PCR analysis (Fig. S1*A*). The *FER* gene was first identified as a regulator in the male–female interaction during pollen tube reception (13–15). *FER* was later shown to function in several other growth regulatory pathways, including root hair elongation regulated by auxin and cell growth induced by other hormones (10, 16–18).

We were curious as to whether the opposite patterns of regulation of FER gene expression by auxin and ABA, two antagonizing hormones in cell growth (2), may implicate a role of FER in both auxin and ABA signaling pathways. To follow up on this possibility, we examined ABA responses of *fer* mutants to determine whether disruption of FER function impacts ABA sensitivity. Three *FER* mutants were analyzed: two null mutants (*fer-4* and *srn*) and a truncated allele called *fer-5* that shows a partial defect in FER function (10). When germinated on Murashige and Skoog (MS) medium supplemented with ABA, *fer-4* and *srn* seedlings showed dramatic growth arrest and turned brown in response to ABA (Fig. 1 *A a* and *b*, *B*, and *C*), whereas the wild-type (WT) and *fer-5* seedlings grew well and remained green. In the absence of exogenous ABA, cotyledons of all five genotypes were expanded and green. When supplemented with 0.25 μM ABA, both *fer-4* and *srn* failed to produce true leaves and eventually died (Fig. 1 *Ab* and *C*).

Author contributions: F.Y., L.Q., L.C., D.L., and S.L. designed research; F.Y., L.Q., C.N., Q.D., X.L., C.L., H.L., C.H., and L.L. performed research; Q.D., D.K., K.L., and A.Y.C. contributed new reagents/analytic tools; F.Y., L.Q., C.N., Q.D., K.L., B.B.B., L.C., A.Y.C., D.L., and S.L. analyzed data; and F.Y., B.B.B., L.C., A.Y.C., D.L., and S.L. wrote the paper.

The authors declare no conflict of interest.

[1]Present address: Institute of Biological, Rural and Environmental Sciences, Aberystwyth University, Aberystwyth, Ceredigion SY23 3EB, United Kingdom.

[2]Present address: Division of Infectious Diseases, Children's Hospital, Harvard Medical School, Boston, MA 02115.

[3]To whom correspondence may be addressed. E-mail: view@berkeley.edu, chenliangbi@126.com, dongbing_lee@yahoo.com.cn, or sluan@berkeley.edu.

This article contains supporting information online at www.pnas.org/lookup/suppl/doi:10.1073/pnas.1212547109/-/DCSupplemental.

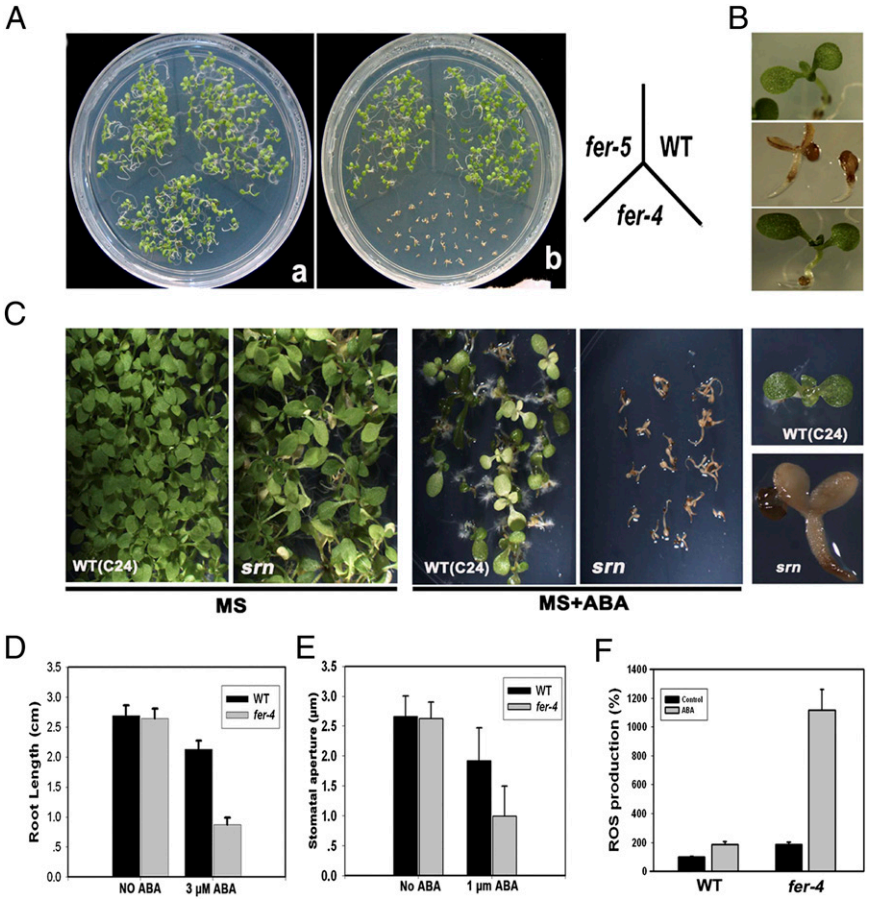

Fig. 1. Hypersensitive ABA responses of *fer* mutant plants. (*A*–*C*) ABA sensitivity in seedlings. Approximately 150 seeds from four independent seed lots of simultaneously grown WT (Columbia-0 and C24), *fer-4*, *fer-5*, and *srn* mutants were sown on agar plates supplemented with ABA (mixed isomers; Sigma-Aldrich A1049). (*A*) The images of plants were taken on day 9 after germination on MS agar medium supplemented with 0 μM (*a*) or 0.25 μM ABA (*b*). (*B*) Close-up images show Col-0 WT (*Top*), *fer-4* (*Middle*), and *fer-5* (*Bottom*) seedlings taken from *Ab*. (*C*) Images indicate *srn* mutant and WT C24 plants on day 8 after germination on MS agar medium supplemented with 0 μM (MS) or 0.5 μM ABA (MS+ABA). (*D*) ABA-induced growth inhibition in roots. Five-day-old seedlings grown on the MS medium were transferred to MS medium containing 3 μM ABA. Root length was measured 4 d after transfer. Each data point is the average ± SE of three independent experiments with 10 plants each. (*E*) Stomatal aperture before and after ABA treatment of *fer-4* and WT leaves. Data are presented as average ± SE of three replicates with 10 apertures each. Three independent experiments yielded similar results. (*F*) Quantification of ROS production in guard cells of the WT and *fer-4* plants after ABA treatment. Confocal fluorescence intensities were quantified as average pixel intensities in three random regions of each guard cell by using the OLYMPUS FV1000 software. The relative ROS production of each treatment was normalized to untreated WT (100%). Data are average values ± SE of nine guard cells per genotype in one experiment. Four independent experiments were conducted with similar results.

We examined the *fer-4* mutant in comparison with the WT in the ABA-inhibited growth assay. Without ABA, the primary root growth of WT and *fer-4* was largely comparable. However, when supplemented with 3 μM ABA, root growth in *fer-4* seedlings was significantly decreased compared with WT ($P < 0.0001$) (Fig. 1*D*). This assay and the one described immediately above demonstrate that the inhibition of growth by ABA was dramatically enhanced in the *fer* mutants.

We then determined whether ABA-induced environmental responses such as stomatal closure are altered in *fer* mutants. We performed stomatal assays using isolated rosette leaves from *fer-4* and WT plants. Maximum stomatal opening was observed when WT intact rosette leaves were floated on stomata-opening buffer and illuminated for 3 h. The same treatment induced maximal aperture of *fer-4* mutants in 6 h, indicative of slower stomatal opening. After maximal aperture was achieved in both the WT and *fer-4* mutant, samples were exposed to 1 μM ABA for 1 h, and stomatal apertures were again measured. Fig. 1*E* shows that stomatal opening in the *fer-4* mutant was more sensitive to ABA than the WT ($P < 0.0001$).

FER May Regulate Reactive Oxygen Species (ROS)-Mediated ABA-Signaling Pathway. Previous work showed that FER regulates auxin-stimulated ROS accumulation in the root and root hair (10), as well as in the leaf under fungal invasion (19). Ample evidence supports a role for ROS as a second messenger in the ABA signaling pathway (20–22). It is possible that FER may regulate ROS accumulation in the ABA response. Because the *FER* mutation caused ABA hypersensitivity in stomatal closing, we analyzed the accumulation of ROS in guard cells. We found higher levels of ROS in the *fer-4* guard cells either in the absence or presence of exogenous ABA (Fig. 1*F*). Whereas ROS accumulation in the WT plants increased 87% after 45-min treatment with 25 μM ABA (from 286.032 ± 46.340 to 535.530 ± 38.618), the same treatment resulted in a 500% increase in ROS levels in the *fer-4* mutant (from 525.041 ± 80.119 to 3188.611 ± 413.820) (Fig. 1*F* and Fig. S1*G*). From these data, we suggest that ABA hypersensitivity of *fer-4* guard cells may be caused, at least in part, by increased ROS production compared with WT.

ROP11/ARAC10 Interacted with GEF1, GEF4, GEF10, and ABI2. Duan et al. (10) reported that FER directly interacts with guanine nucleotide exchange factors (RopGEF) to activate GTPase (ROP/ARAC) in response to auxin. Furthermore, some ROPs, such as ROP10 and ROP6, have been shown to negatively regulate ABA responses (23, 24). It is possible that FER may regulate ABA responses through activation of some ROPs/ARACs that interact with components in the primary ABA signaling pathway involving the PYR/PYL/RCAR receptors, A-type PP2Cs, and SnRK2s. To test this hypothesis, we carried out yeast two-hybrid (Y2H) assays to identify physical interactions among FER, GEFs, ROPs, A-type PP2Cs, and SnRK2s. It has been shown that FER interacts with the five GEFs that function as activators of ROPs (10). We used the FER-interacting GEFs to further identify ROPs/ARACs. Among the interactions, we found that ROP11/ARAC10 interacted not only with GEF1, GEF4, and GEF10—three of the FER-interacting GEFs—but also with ABI2, one of the A-type PP2Cs (Fig. 2 *A* and *B*). We confirmed the interaction between ROP11/ARAC10 and ABI2 in planta by a bimolecular fluorescence complementation (BiFC) assay (Fig. 2*C*). We further found that both the WT (WT-ROP11/ARAC10) and constitutively active (CA) form of ROP11/ARAC10 (CA-ROP11/ARAC10), but not the dominant negative (DN) form of ROP11/ARAC10 (DN-ROP11/ARAC10), interacted with ABI2 (Fig. 2*A*). Together, our

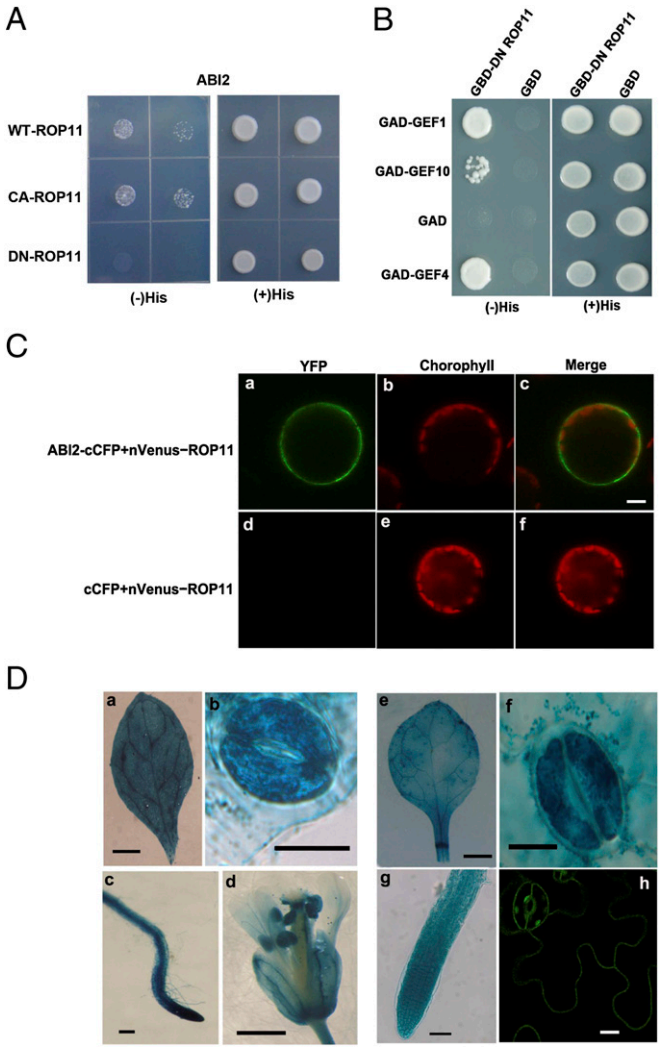

Fig. 2. ROP11/ARAC10 interactions with GEFs and ABI2 and expression patterns of *ROP11/ARAC10*, *GEF1*, and *FER*. (*A*) Y2H assays showing WT or CA-ROP11/ARAC10, but not DN-ROP11/ARAC10, interacting with ABI2. (*B*) DN-ROP11/ARAC10 interacts with full-length GEF1, GEF4, and GEF10 in the Y2H assays. (*C*) ROP11/ARAC10 and ABI2 interacted in BiFC assays in *Arabidopsis* protoplasts. (*a*) Interacting nVenus–ROP11/ARAC10 and ABI2–cCFP was observed as GFP image. (*d*) Negative control (nVenus–ROP11/ARAC10 with cCFP vector) was shown. (*b* and *e*) Chloroplasts are indicated by red auto-fluorescence. (*c* and *f*) Merged images of GFP and red signals are shown. (Scale bars: 10 μm.) (*D a–d*) The expression of *ROP11/ARAC10–GUS* reporter in leaves (*a*), guard cells (*b*), roots (*c*), and pollen (*d*). (*e–g*) GEF1–*GUS* expression was also detected in leaves (*e*), guard cells (*f*), and roots (*g*). (*h*) Pro*FER-FER-GFP* was expressed in epidermal and guard cells. (Scale bars: *b–d*, *f*, and *g*, 20 μm; *a* and *e*, 0.5 cm).

data suggest that the GTP-binding form, but not the GDP-binding form, of ROP11/ARAC10 interacted with ABI2 (Fig. 2*A*). These results suggest that the interaction of ROP11/ARAC10 with ABI2 occurs after activation by FER–GEFs and may serve as a cross-talk mechanism between the FER pathway and the primary ABA signaling pathway.

Interestingly, although ROP10 and ROP11/ARAC10 are similar in amino acid sequence, and both function in ABA responses, ROP10 did not interact with ABI2 in the Y2H and in BiFC assays, suggesting that ROP10 may regulate ABA responses through different partner proteins and pathways. Indeed, mutation in either ROP10 or ROP11 causes ABA hypersensitivity in mutant plants (23) (Fig. 3), consistent with the idea that they are not functionally redundant.

We next analyzed the expression patterns of *ROP11/ARAC10* and found that *ROP11/ARAC10* was highly expressed in stomatal guard cells and several other tissues (Fig. 2*D a–d*). This expression pattern coincided with those for *FER* and *GEF1* (Fig. 2*D e–h* and ref. 10), making it possible for these genes to work together in responses to ABA.

ROP11/ARAC10 Can Activate the Phosphatase Activity of ABI2. We next examined the biochemical consequence of the ROP11/ARAC10–ABI2 interaction by measuring the phosphatase activity of ABI2 in the presence and absence of ROP11/ARAC10. As shown in Fig. 3*A*, the WT ROP11/ARAC10 and CA-ROP11/ARAC10 loaded with GTP-γ-S activated ABI2 phosphatase ($P < 0.0001$), but the DN-ROP11/ARAC10 loaded with GDP did not (Fig. 3*A*). Another ROP/ARAC, ROP10, also failed to interact with ABI2 or activate its phosphatase activity in the presence of GTP-γ-S. In the ABA signaling pathway, ABI2, as one of the A-type PP2Cs, inhibits the SnRK2.6/OST1 kinase activity (3–5). If ROP11/ARAC10 enhances ABI2 activity, the presence of ROP11/ARAC10 should further reduce the kinase activity of OST1. In a kinase assay, the activity of OST1 was reduced by the addition of ABI2, consistent with earlier studies. Adding ABI2 together with ROP11/ARAC10 further reduced kinase activity (Fig. 3*B*). OST1 activity was not affected by ROP11/ARAC10 in the absence of ABI2, confirming that ROP11/ARAC10 inhibits ABA signaling through activation of the negative regulator ABI2.

***rop11/arac10* Mutants Were Hypersensitive to ABA.** If ROP11/ARAC10 interacts with ABI2, thereby activating its phosphatase activity, the *rop11/arac10* mutant, like the *fer* mutant, should be hypersensitive to ABA. To pursue this possibility, we isolated three mutant alleles of *ROP11/ARAC10* for ABA response analysis: *rop11/arac10-1*, Salk_039681; *rop11/arac10-2,* Salk_087260C; and *rop11/arac10-3*, Salk_063154 (Fig. S1 *B* and *C*). We found that all three mutants were hypersensitive to ABA in the seed germination assay (Fig. 3*E* and Fig. S1 *D–F*). In addition, *rop11/arac10* mutants resembled *fer-4* in being hypersensitive to ABA in the seedling growth assay (Fig. 3*D a–f* and Fig. S1*D*). Finally, when the *rop11/arac10* mutants were analyzed in the root growth and stomatal assays, they resembled *fer-4* in displaying increased sensitivity to ABA ($P < 0.0001$) (Fig. 3 *C* and *F* and Fig. S1*E*).

***gef1/4* Double and *gef1/4/10* Triple Mutants Were Hypersensitive to ABA.** To confirm the role for the FER–GEF1/4/10–ROP11–ABI2 pathway in the ABA response, we analyzed this property in null mutants of *gef1* (GK_586B11), *gef4* (Salk_107520), and *gef10* (Salk_009456) and found no difference in these single mutants compared with WT (Fig. 4 *A* and *B*), suggesting functional redundancy of the three *GEF* genes. By contrast, when the *gef1/4* double and *gef1/4/10* triple mutants were isolated and examined in the same assays, they displayed ABA hypersensitivity in both the root growth and stomatal assays. Furthermore, the *gef1/4/10* triple mutant showed a stronger phenotype compared with the *gef1/4* double mutant (Fig. 4 *A* and *B*). This result suggests that these three GEFs interact with FER and ROP11/ARAC10 and share functions in relaying the FER signal in responding to ABA.

Concluding Remarks

We have identified a pathway linked to the FER receptor kinase that negatively regulates ABA responses through activation of an A-type PP2C phosphatase, ABI2. In the absence of ABA, the phosphatase interacts and inhibits an SnRK2-type protein kinase that acts as a positive regulator of ABA responses. Increased levels of ABA induce an interaction of PP2C with PYR/PYL/RCAR receptors that triggers release of active SnRK2s, thereby activating downstream targets (25–27). These targets include

PLANT BIOLOGY

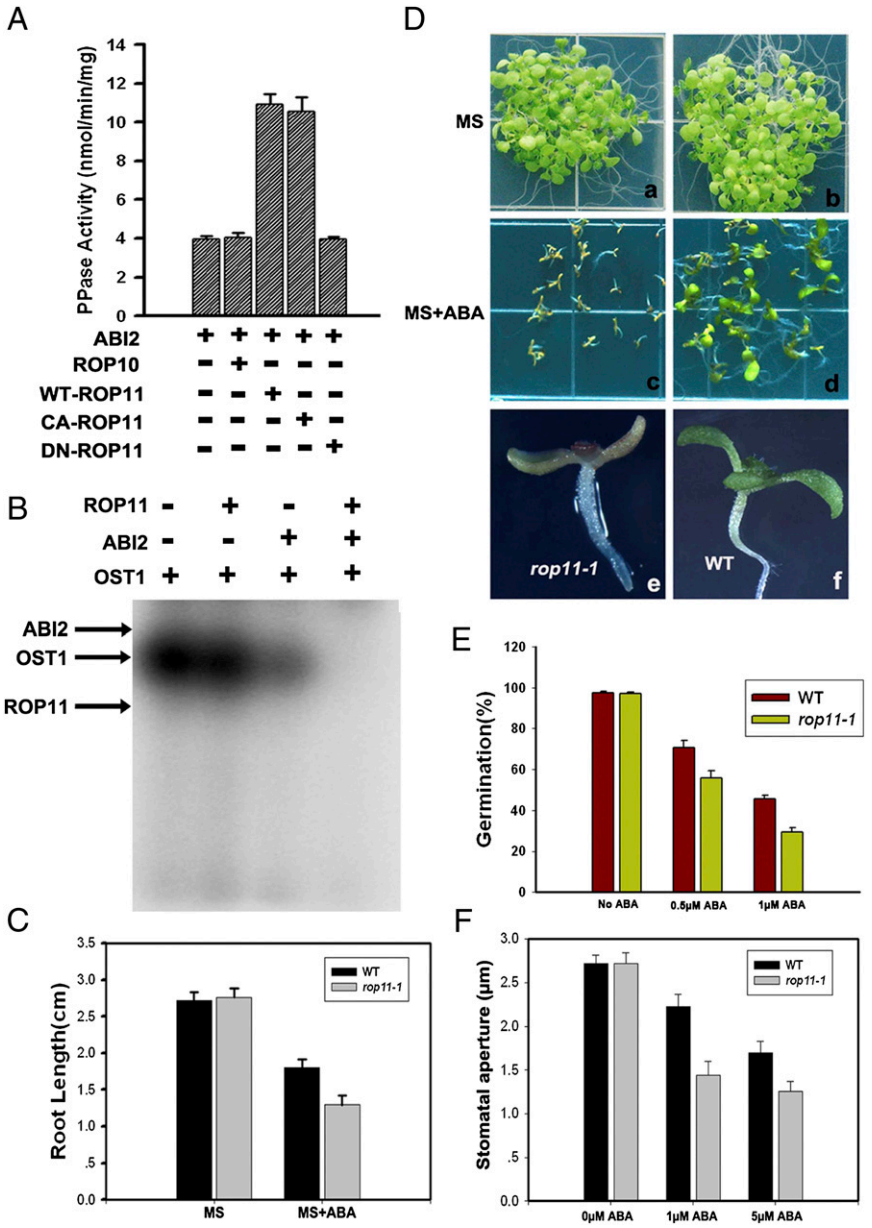

Fig. 3. ROP11/ARAC10 activates ABI2 phosphatase, and *rop11/arac10* mutants are ABA-hypersensitive. (*A*) ROP11/ARAC10 enhances phosphatase activity of ABI2. Phosphopeptide phosphatase assays were conducted as described in *Materials and Methods*. Data are presented as average activity ± SE of three replicates in one experiment. Three independent experiments were conducted with similar results. (*B*) OST1 kinase activity was inhibited by ROP11/ARAC10–ABI2. Equal amount of OST1 was added to individual kinase reactions in the presence of other factors indicated at the top of the autoradiography picture. The proteins and their positions on the gel are indicated by arrows on the left. The radioactive band resulted from OST1 autophosphorylation (25). (*C*) ABA-induced growth inhibition in roots. Five-day-old seedlings grown on MS medium were transferred to MS containing 9 μM ABA, and root length was measured 10 d after transfer. Each data point represents the average length ± SE of three experiments with 10 seedlings each. (*D*) ABA-induced growth arrest in *rop11/arac10-1* seedlings. Col-0 and *rop11/arac10-1* (SALK_039681) were grown and harvested at the same time. (*a*–*d*) Sterilized seeds were plated on MS medium supplemented with 0 μM (*a* and *b*) or 2 μM ABA (*c* and *d*) at 23 °C for 9 d before photographing. (*e* and *f*) Close-up pictures of *rop11/arac10-1* (*e*) and WT (*f*) show difference in ABA-induced growth arrest. Experiment was conducted five times with similar results. (*E*) ABA inhibition of germination in the WT and *rop11/arac10-1* seeds. Approximately 100 seeds from three independent seed lots of simultaneously grown WT and mutant plants were germinated on different concentrations of ABA. The germination percentage was calculated 2 d after the seeds were plated on MS medium. The experiment was replicated three times. Each value is the average ± SE of three replicates. (*F*) Stomatal response to ABA. Stomatal apertures were measured with WT and *rop11/arac10-1* plants. Data are presented as average value ± SE of three replicates with 10 apertures each. Four independent experiments were conducted with similar results.

transcription factors that activate ABA-responsive gene expression (8), ion channels that regulate guard cell turgor and stomatal aperture (25, 28), and enzymes that control the production of ROS (29). The A-type PP2Cs and SnRK2s are partitioned in multiple subcellular locations, including the nucleus, cytosol, and plasma membrane, thus enabling them to regulate targets present in different compartments of the cell. Although the FER receptor kinase positively regulates the auxin response in the growth of roots and root hairs (10), the present results suggest that FER–RopGEF–ROP/ARAC modules negatively regulate

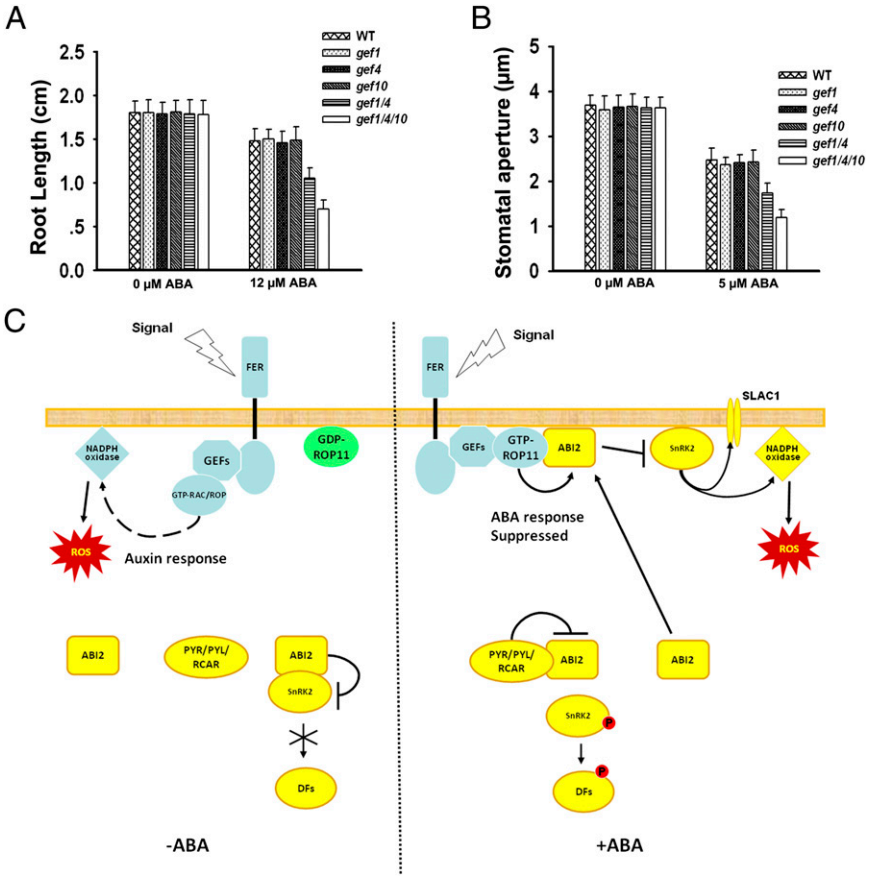

Fig. 4. ABA response of *gef* mutants and a working model for the FER signaling pathway in the regulation of ABA responses. (*A*) ABA-induced growth inhibition in roots. The WT, single mutants, *gef1/4* double mutant, and *gef1/4/10* triple mutant were grown on MS medium for 5 d before transfer to MS containing 12 μM ABA. Root length was then measured 3 d after transfer. Each value is the average ± SE of three replicates of 30 plants. Three separate experiments were conducted. (*B*) ABA-induced stomatal closure in WT and *gef* mutants. Leaves were treated with 5 μM ABA for 1 h before stomatal apertures were measured. Each value is the average ± SE of 3 independent experiments with 10 apertures each. (*C*) Working model for FER pathway in regulating response to ABA. The FER–GEF–ROP/ARAC pathway is an essential module for the auxin response in cell growth. ABI2 is a major component of ABA signaling pathway. The ROP11/ARAC10–ABI2 interaction mediates cross-talk between the auxin and ABA signals. Arrows denote activation, and bars indicate repression. Details are described in the text.

ABA responses, thus serving as a cross-talk node for antagonizing the ABA response by the auxin signaling pathway.

We propose that the FER–RopGEF1/4/10–ARAC10/ROP11 pathway channels a signal to activate ABI2 that, in turn, inhibits the SnRK2-mediated ROS production characteristic of the ABA response (Fig. 4*C*). Disruption of the FER pathway lowers ABI2 activity and leads to hyperactivation of the SnRK2s with consequent elevated levels of ROS production. The increased ROS induces stomatal closure, cell death, and growth inhibition as reflected in ABA-induced seedling arrest and root inhibition. It is possible that ion channels such as SLAC1 located in the plasma membrane participate in this cross-talk and also function in the stomatal response.

Materials and Methods

Phenotype and ROS Analyses. *Arabidopsis thaliana* plants were grown in a room with constant temperature at 23 °C under 16-h-light/8-h-dark cycles. Seeds for the T-DNA insertion lines were purchased from the *Arabidopsis* Biological Resource Center and the GABI-Kat collections, and the double and triple mutants were obtained by crosses of single mutants. *Arabidopsis* seeds were surface-sterilized and germinated on 1/2 MS medium supplemented with 1% sucrose and solidified with 0.9% agar. ABA (mixed isomers; Sigma-Aldrich A1049) or an equal volume of ethanol as a control was added to the medium to the concentrations indicated in the figure legends.

For stomatal aperture assays, leaves were floated on stomatal opening buffer (5 mM Mes, 5 mM KCl, 50 μM $CaCl_2$, pH 5.6) under light for the indicated time and then treated with ABA for 1 h. Thereafter, stomatal apertures were measured as described (30). ROS measurements were performed in guard cells essentially as described (30). Briefly, epidermal tissues were incubated for 3 h in a buffer containing 30 mM KCl and 10 mM Mes–KOH, pH 6.15. Then, 30 μM 2′,7′-dichlorodihydro-fluorescein diacetate (Sigma) was added to the incubation buffer. After 20-min incubation, the dye was removed by three washes with distilled water. Epidermal tissues were incubated for 45 min with 25 μM ABA or equal volume of ethanol as a control. The fluorescence was detected by using a confocal microscope (OLYMPUS FV1000) with 488-nm excitation light.

All statistical analyses were carried out by using SigmaPlot software (Systat Software). The corresponding *P* values were determined by applying the Student *t* test (paired *t* test) comparing data from the two groups.

Gene Expression Studies. Total RNA was prepared with TRIzol (Invitrogen) from mixed tissues of 10-d-old *Arabidopsis* seedlings grown under long-day conditions after treatment with H_2O, 1 μM indole-3-acetic acid, or 10 μM ABA for 1 h. Two micrograms of total RNA was reverse-transcribed to cDNA (Invitrogen) after DNase treatment (17); the primers used in these experiments are shown in Table S1. For β-glucuronidase (GUS) expression analysis, the promoter region containing the ATG start codon of *ROP11/ARAC10* and *GEF1* were amplified (primers are shown in Table S1) and cloned into the binary vector pBI101.2 to produce the translational fusion with the GUS gene. The resultant constructs were transformed into *Arabidopsis* (Col-0) plants, and nine independent transgenic lines were analyzed with GUS staining (31). The ProFER–FER–GFP fusion transgenic lines were described (10). Two-week-old leaves were used to examine the FER–GFP localization in the epidermal and guard cells using confocal microscope (OLYMPUS FV1000) with 488-nm excitation light.

Protein–Protein Interaction Analysis. Full-length cDNA sequences of the *PP2CAs* were subcloned into the pGADT7 vector by using the primers described in Table S1, cotransformed into yeast cells AH109, and plated on synthetic dropout medium (SD/–Trp–Leu–His) supplemented with 10 mM 3-aminotriazole for 1 wk (31).

According to a ROP10 study, mutations Q66L and D123A in the ROP10 protein produce a CA and a DN form of ROP10, respectively (23). The same mutations in ROP11/ARAC10 were made to produce CA-ROP11/ARAC10 and DN-ROP11/ARAC10 by using PCR-based site-directed mutagenesis. Two primers (ROP11–CD-F and ROP11–CD-R) were used to amplify the full-length coding region of *ROP11/ARAC10*. Two mutagenesis primer pairs (ROP11–CA-TF paired with ROP11–CA-TR and ROP11–DN-TR paired with ROP11–DN-TF) were used to produce Q66L and D123A mutations, respectively. The coding

regions of *ROP11/ARAC10*, *CA-ROP11/ARAC10* and *DN-ROP11/ARAC10* were subcloned to the pGBKT7 separately. The primers are listed in Table S1.

The ORF sequences of *ROP11/ARAC10* and *PP2CAs* were amplified by PCR and cloned into plasmids pE3228 and pE3449, respectively, for BiFC assays in mesophyll protoplasts (32). Protoplasts were isolated from 5-wk-old *Arabidopsis* rosette leaves essentially as described (33). Leaf strips were incubated in the cell wall-degrading enzyme solution in the dark for 3.5 h. Protoplasts were purified (33) and transfected with 20 μg of plasmid DNA and an equal volume of PEG solution. The transfected protoplasts were incubated in the dark at 23 °C for 16 h to allow expression of the BiFC proteins. Fluorescence was detected with a confocal microscope (LSM 5 LIVE; Zeiss) using an excitation wavelength of 488 nm.

ABI2 and OST1 Enzyme Assays. The coding DNA sequences of *ROP10*, *ROP11/ARAC10*, and *ABI2* were amplified by PCR and cloned into pGEX4T-1 (Amersham Biosciences) expression vector. All constructs were transformed into BL21(DE3) for protein expression according to a described procedure (25). Proteins were purified as GST fusions by using immobilized glutathione according to instructions of the manufacturer (Pierce). The glutathione solution containing ABI2 was concentrated and dialyzed vs. a buffer containing 50 mM imidazole (pH 7.2) and 5 mM $MgCl_2$. The recombinant ROP10, ROP11/ARAC10, CA-ROP11/ARAC10, and DN-ROP11/ARAC10 were first incubated with 10 mM EDTA for 5 min at room temperature, and then the GTPases were loaded with 10 mM GTP-γ-S (Sigma; G8634) or 10 mM GDP (Sigma; G7127) for 20 min at room temperature, followed by the addition of 40 mM $MgCl_2$. Loaded proteins were washed four times in 50 mM imidazole (pH 7.2) and 5 mM $MgCl_2$.

Phosphatase activity was measured by using the Ser/Thr Phosphatase assay kit (Promega; V2460) as described (6). Reactions were performed in a 50-μL volume containing 9 μg of GST–ABI2, in the presence of other factors, including 10 μg of GST–ROP11/ARAC10, GST–CA-ROP11/ARAC10, GST–DN-ROP11/ARAC10, or GST–ROP10. After incubation with the RRA(phosphoT)VA peptide substrate in 50 mM imidazole (pH 7.2), 5 mM $MgCl_2$, 0.5 μg/mL BSA, and 0.1% β-mercaptoethanol for 40 min at room temperature, the reaction was stopped by adding 50 μL of molybdate dye. After incubation for an additional 20 min at room temperature, absorbance was measured at 600 nm.

For OST1 kinase assays, GST–OST1 was expressed and purified as described (25). The kinase buffer contained 20 mM Tris·HCl (pH 7.5), 2.5 mM $MnCl_2$, 2.5 mM $MgCl_2$, 1 mM $CaCl_2$, 1 mM DTT, and 1× Roche EDTA free proteinase inhibitors. The protein combinations indicated in the legend of Fig. 3 were included in a total volume of 20 μL. The reaction was started by adding [^{32}P] ATP. After incubation for 45 min at 30 °C, the reaction was stopped by adding 4 μL of 6× loading buffer and then separated by SDS/PAGE using a 12% (wt/vol) SDS–acrylamide gel. ^{32}P was detected by autoradiography using a Typhoon imager (Molecular Dynamics).

Note. When this paper was under preparation, another group reported that ROP11 interacted with ABI1 and regulated ABA responses (34, 35), although authors found that ABI1 interaction with ROP11 occurs when the regulatory domain of ABI1 is deleted (35). It seems likely that different cross-talk nodes are present in subcellular compartments, such as the nucleus and cytosol, where they link alternate signals to ABA. Further work should highlight the importance of these cross-talk nodes in hormonal interactions that control plant growth and development.

ACKNOWLEDGMENTS. We thank Drs. Stanton Gelvin and Lan-Ying Lee for BiFC vectors; Drs. Xianyong Sheng and Lei Guo for assistance in laser confocal analysis; and He Lei and Qingbo Li for their support. This work was supported by National Science Foundation of China Grants NSFC-31170229 and 30970273, National High Technology Research and Development Program of China Grant 2010AA101305, Key Program for Science and Technology of Hunan Province Grant 2009FJ1004-1,2, the National Science Foundation [S.L., Hen-Ming Wu (University of Massachusetts), and A.Y.C.]. C.N. was supported by a Fundação para a Ciência e Tecnologia (Portugal) doctoral scholarship and a University of Massachusetts Plant Biology Graduate Program Gilgut Fellowship.

1. Bellandi DM, Dorffling K (1974) Effect of abscisic acid and other plant hormones on growth of apical and lateral buds of seedlings. *Physiol Plant* 32:369–372.
2. Pilet PE (1989) Differential growth and hormone redistribution in gravireacting maize roots. *Environ Exp Bot* 29:37–45.
3. Raghavendra AS, Gonugunta VK, Christmann A, Grill E (2010) ABA perception and signalling. *Trends Plant Sci* 15:395–401.
4. Cutler SR, Rodriguez PL, Finkelstein RR, Abrams SR (2010) Abscisic acid: Emergence of a core signaling network. *Annu Rev Plant Biol* 61:651–679.
5. Hubbard KE, Nishimura N, Hitomi K, Getzoff ED, Schroeder JI (2010) Early abscisic acid signal transduction mechanisms: Newly discovered components and newly emerging questions. *Genes Dev* 24:1695–1708.
6. Park SY, et al. (2009) Abscisic acid inhibits type 2C protein phosphatases via the PYR/PYL family of START proteins. *Science* 324:1068–1071.
7. Ma Y, et al. (2009) Regulators of PP2C phosphatase activity function as abscisic acid sensors. *Science* 324:1064–1068.
8. Fujii H, et al. (2009) In vitro reconstitution of an abscisic acid signalling pathway. *Nature* 462:660–664.
9. Nishimura N, et al. (2009) Structural mechanism of abscisic acid binding and signaling by dimeric PYR1. *Science* 326:1373–1379.
10. Duan Q, Kita D, Li C, Cheung AY, Wu HM (2010) FERONIA receptor-like kinase regulates RHO GTPase signaling of root hair development. *Proc Natl Acad Sci USA* 107: 17821–17826.
11. Shiu SH, Bleecker AB (2001) Receptor-like kinases from *Arabidopsis* form a monophyletic gene family related to animal receptor kinases. *Proc Natl Acad Sci USA* 98: 10763–10768.
12. Chae L, Sudat S, Dudoit S, Zhu T, Luan S (2009) Diverse transcriptional programs associated with environmental stress and hormones in the *Arabidopsis* receptor-like kinase gene family. *Mol Plant* 2:84–107.
13. Huck N, Moore JM, Federer M, Grossniklaus U (2003) The *Arabidopsis* mutant *feronia* disrupts the female gametophytic control of pollen tube reception. *Development* 130:2149–2159.
14. Escobar-Restrepo JM, et al. (2007) The FERONIA receptor-like kinase mediates male-female interactions during pollen tube reception. *Science* 317:656–660.
15. Rotman N, et al. (2003) Female control of male gamete delivery during fertilization in *Arabidopsis thaliana*. *Curr Biol* 13:432–436.
16. Nibau C, Cheung AY (2011) New insights into the functional roles of CrRLKs in the control of plant cell growth and development. *Plant Signal Behav* 6:1–5.
17. Guo H, et al. (2009) Three related receptor-like kinases are required for optimal cell elongation in *Arabidopsis thaliana*. *Proc Natl Acad Sci USA* 106:7648–7653.
18. Deslauriers SD, Larsen PB (2010) FERONIA is a key modulator of brassinosteroid and ethylene responsiveness in *Arabidopsis* hypocotyls. *Mol Plant* 3:626–640.
19. Kessler SA, et al. (2010) Conserved molecular components for pollen tube reception and fungal invasion. *Science* 330:968–971.
20. Kwak JM, et al. (2003) NADPH oxidase *AtrbohD* and *AtrbohF* genes function in ROS-dependent ABA signaling in *Arabidopsis*. *EMBO J* 22:2623–2633.
21. Zhang X, et al. (2001) Hydrogen peroxide is involved in abscisic acid-induced stomatal closure in *Vicia faba*. *Plant Physiol* 126:1438–1448.
22. Cho DS, Shin DJ, Jeon B, Kwak JM (2009) ROS-mediated ABA signaling. *J Plant Biol* 52: 102–113.
23. Zheng Z-L, et al. (2002) Plasma membrane-associated ROP10 small GTPase is a specific negative regulator of abscisic acid responses in *Arabidopsis*. *Plant Cell* 14:2787–2797.
24. Lemichez E, et al. (2001) Inactivation of AtRac1 by abscisic acid is essential for stomatal closure. *Genes Dev* 15:1808–1816.
25. Lee SC, Lan W, Buchanan BB, Luan S (2009) A protein kinase-phosphatase pair interacts with an ion channel to regulate ABA signaling in plant guard cells. *Proc Natl Acad Sci USA* 106:21419–21424.
26. Vlad F, et al. (2009) Protein phosphatases 2C regulate the activation of the Snf1-related kinase OST1 by abscisic acid in *Arabidopsis*. *Plant Cell* 21:3170–3184.
27. Yoshida R, et al. (2006) The regulatory domain of SRK2E/OST1/SnRK2.6 interacts with ABI1 and integrates abscisic acid (ABA) and osmotic stress signals controlling stomatal closure in *Arabidopsis*. *J Biol Chem* 281:5310–5318.
28. Geiger D, et al. (2009) Activity of guard cell anion channel SLAC1 is controlled by drought-stress signaling kinase-phosphatase pair. *Proc Natl Acad Sci USA* 106: 21425–21430.
29. Sirichandra C, et al. (2009) Phosphorylation of the Arabidopsis AtrbohF NADPH oxidase by OST1 protein kinase. *FEBS Lett* 583:2982–2986.
30. Mustilli AC, Merlot S, Vavasseur A, Fenzi F, Giraudat J (2002) Arabidopsis OST1 protein kinase mediates the regulation of stomatal aperture by abscisic acid and acts upstream of reactive oxygen species production. *Plant Cell* 14:3089–3099.
31. Yu F, et al. (2010) ANK6, a mitochondrial ankyrin repeat protein, is required for male-female gamete recognition in *Arabidopsis thaliana*. *Proc Natl Acad Sci USA* 107: 22332–22337.
32. Lee LY, Fang MJ, Kuang LY, Gelvin SB (2008) Vectors for multi-color bimolecular fluorescence complementation to investigate protein-protein interactions in living plant cells. *Plant Methods* 4:24.
33. Kovtun Y, Chiu WL, Tena G, Sheen J (2000) Functional analysis of oxidative stress-activated mitogen-activated protein kinase cascade in plants. *Proc Natl Acad Sci USA* 97:2940–2945.
34. Li Z, Kang J, Sui N, Liu D (2012) ROP11 GTPase is a negative regulator of multiple ABA responses in *Arabidopsis*. *J Integr Plant Biol* 54:169–179.
35. Li Z, et al. (2012) ROP11 GTPase negatively regulates ABA signaling by protecting ABI1 phosphatase activity from inhibition by the ABA receptor RCAR1/PYL9 in *Arabidopsis*. *J Integr Plant Biol* 54:180–188.